Ceramics International **24** (1998) 259–264
PII: S0272-8842(96)00079-X

0272-8842/98 $19.00+.00

Phase Analysis and Role of Microstructure in the Development of High Strength Porcelains

Soumen Maity[a] & B. K. Sarkar[b]

[a]Development Consultants Ltd, 24B Park Street, Calcutta 700 016, India
[b]Department of Material Science, Indian Association for the Cultivation of Science, Jadavpur, Calcutta 700 032, India

(Received 16 March 1996; accepted 29 August 1996)

Abstract: The flexural strength improved from 154 to 196 MPa at 1450°C when the alumina:cordierite ratio was changed from 0 to 4·2, respectively, in a china clay–sillimanite mix. XRD and microscopic analysis of the phases that developed with increasing temperature revealed a microstructure of euhedral grains of sillimanite interspersed with fine mullite needles and a dense glassy phase wetting the crystalline mosaic structure. These contributed to the improved strength. © 1998 Elsevier Science Limited and Techna S.r.l. All rights reserved

1 INTRODUCTION

In recent years the electrical porcelain industry has been seeking insulators for electrical appliances with higher mechanical strengths at reduced cost. The oldest bodies, and those in most common use today, are felspathic porcelains made with clay, quartz and feldspar. They have flexural strengths between 50 and 80 MPa. Higher strengths are achieved by controlling the size of the quartz particles in the range of 10–30 μm.[1–3]

High alumina bodies have been investigated and used extensively since the early 1940s. Substantial increases in strength have been reported;[4] with an alumina content of $>65\%$, they are cost effective. In a study on the structure of porcelains, Schuller[5] reported two morphologies of mullite; one the well-known needles, formed by recrystallization from the glassy phase, and primary mullite. The latter was scaly and formed from silica and alumina liberated by the decomposition of kaolin. Schuller also reported[6] that primary mullite dissolved in the glassy phase of bodies rich in silica, but subsequently recrystallized into needle-shaped, secondary mullite. However, in melts rich in alumina its recrystallization was suppressed.

Petrova and Avgustinik[7] reported that alumina began to dissolve slowly in a feldspar melt at about 1200°C; dissolution of alumina increased with increasing time and temperature. In X-ray diffraction and microstructure studies, Floyd et al.[8] reported that the α-alumina content of alumina porcelain bodies remained virtually unaltered during firing.

In the present investigation, quartz was fully substituted by beach sand sillimanite in all but one of the porcelain compositions. The reason for selecting beach sand sillimanite was two-fold. Firstly, unlike quartz, it is a volume stable material and will not generate excessive stresses in ceramic microstructures. Also, being more fracture resistant than quartz, it might increase the strength by dispersion-strengthening. Finally, beach sand sillimanite is an almost inexhaustable material and opens up an avenue for effective utilization of waste materials.

Feldspar was also substituted by crystallized glass of cordierite ($2MgO{\cdot}2Al_2O_3{\cdot}5SiO_2$) composition to improve the strength of the fired body. To furthur improve the strength, the crystallized glass was progressively replaced by alumina. X-ray analysis and microstructural investigations were carried out to elucidate the effect of compositional variation.

2 EXPERIMENTAL PROCEDURE

2.1 Raw materials

Raw materials used in the present investigation were china clay, feldspar (Rajmahal, Bihar); talc (Jaipur, Rajasthan); quartz (Ranchi, Bihar), calcined alumina (INDAL Co. Ltd), beach sand sillimanite, a by-product obtained from zircon (etc.) separation, from beach sand in Kerala, and reagent grade TiO_2. All the above materials were procured in ground form, at least −250 mesh (75 μm). Chemical analysis of the raw materials is shown in Table 1.

2.2 Crystallized glass preparation

The glass-ceramic used in the present investigation was essentially of cordierite composition, belonging to the $MgO–Al_2O_3–SiO_2$ system. Raw materials consisting of 37% china clay, 32% talc, 12% feldspar, 9% calcined alumina and 10% TiO_2, were melted for 2 h in sillimanite crucibles at 1450°C. The melt was further furnace cooled to room temperature to permit nucleation and growth of crystalline phases. The crystallized glass was crushed, ground and finally powdered to −300 mesh (50 μm) prior to further use.

XRD analysis of the crystallized glass revealed the principal crystalline phase to be α-cordierite with minor amounts of quartz, mullite, cristobalite, rutile and Mg–Al spinel. A small amount of glassy phase also remained due to incomplete crystallization. The crystallized glass will be abbreviated as CGC. Some of the unreacted TiO_2 (added as a nucleating agent) also remained, in the form of rutile.

2.3 Sample preparation

The compositions shown in Table 2 were mixed and wet milled in porcelain pots for 20 h with porcelain grinding media. The resultant slurries were passed over a magnetic separator to remove iron contamination and sieved to pass −300 mesh (50 μm). Batch compositions were uniaxially pressed, in the form of rectangular bars, and fired between 1300° and 1450°C at a heating rate of 50°C/h with a soaking time of 2 h. Batches were furnace cooled prior to further use.

2.4 Measurement

The major crystalline phases were identified by XRD; microstructural features were studied by polarizing and scanning electron microscopy (SEM).

XRD analyses were carried out using a PW-1730 X-ray unit with a diffractometer, pulse height analyser and proportional counter. Ni-filtered CuK_α radiation was used for the experiment. The tube was run at 40 kV and 20 mA.

Thin sections were viewed under transmitted light in a polarizing microscope Ortholux II, POL-BK (Leitz, Germany).

For analysis of phase assemblages and morphology, specimens were mirror-polished and etched in 5% HF solution for 30 s. After cleaning ultrasonically in acetone, they were carbon coated. Images were taken both under secondary (SE) and back scattered electron (BSE) mode. Phase assemblages were identified by X-ray elemental mapping and microprobe analysis. SEM and SEPMA (scanning electron probe micro-analysis) were carried out in a

Table 1. Chemical analysis of raw materials

Constituents (wt%)	China clay	Feldspar	Talc	Quartz	Calcined alumina	Sillimanite	Titania
SiO_2	47.63	65.63	63.29	99.06	0.09	37.50	0.38
Al_2O_3	37.89	19.19	0.76	0.30	99.93	59.78	Tr
Fe_2O_3	0.56	0.17	0.39	0.19	0.06	0.37	0.27
CaO	0.48	Tr	Tr	0.23	Tr	0.52	0.32
MgO	0.13	0.49	31.56	Tr	Tr	0.50	0.34
Na_2O	0.10	3.56	0.82	0.06	0.05	0.07	0.10
K_2O	0.18	10.42	0.06	0.09	—	0.04	0.26
TiO_2	0.61	Tr	Tr	Tr	Tr	0.76	98.01
L.O.I	12.42	0.65	1.80	0.28	—	0.30	0.32

Table 2. Raw material composition (wt%) used in the batches

Raw material	Batch				
	S_{15}	A_0	A_{10}	A_{15}	A_{20}
China clay	50	50	50	50	50
Sillimanite sand	25	25	25	25	25
Cordierite glass-ceramic	15	25	15	10	5
Alumina	—	—	10	15	20
Quartz	10	—	—	—	—

carried out in a Camebax-Micro (Cameca, France) using an accelerating voltage of 15 kV. The beam current for elemental mapping was 2 mA and for analysis 60 mA. Analyses were performed for Al, Si, Mg and Ti. For mapping and elemental analyses, the following spectral lines and crystals were taken as standards:

Element	Spectral lines	Crystal
Al	$K\alpha_1$	TAP
(Thallium acid phthalate)		
Si	$K\alpha_1$	TAP
Mg	$K\alpha_1$	TAP
Ti	$K\alpha_1$	PET
(Pentacrythrilol)		

The counting time for each analysis was 5 s. Ten readings were taken for each analysis and the average recorded.

3 RESULTS AND DISCUSSION

3.1 Phase analysis

The principal raw materials consisted of 50% china clay, 25% sillimanite sand with cordierite glass-ceramic (CGC) and alumina in varying proportions. Firing temperatures for attaining vitrification were 1300 (S_{15}, A_0), 1350 (A_{10}), 1400 (A_{15}) and 1450°C (A_{20}), with a soaking time of 2 h at the respective temperatures.

The major phases present in the fired samples were sillimanite, mullite, cordierite and a siliceous glass. The minor phases present were quartz, rutile and corundum (Fig. 1).

Since the highest intensity peaks of mullite and sillimanite merged, no quantitative phase estimation could be made. However, as the quantity of sillimanite sand added was the same in all the compositions (25%), changes in the peak intensity were primarily due to the crystallization of mullite.

With progressive replacement of CGC by alumina, increased formation of mullite took place, even at 1450°C, as evidenced from the comparative change in peak heights at 3·42 Å and 3·39 Å (Fig. 1). Since the clay content of all the compositions was the same, increased mullite formation is attributed to dissociation of sillimanite. At lower firing temperatures (1300°C), mullite formation was less (S_{15}, A_0) compared to other samples. In these samples, mullite formed mainly from dissociation of clay.

Cordierite was detected in samples where CGC was added in greater quantity (≥15%) and fired to 1300°C (S_{15}, A_0). Above 1300°C, the crystallized cordierite was completely reacted, as evident by the absence of any cordierite peak at 8·50°; samples A_{10}, A_{15} and A_{20} (Fig. 1).

Minor quartz and rutile were detected in S_{15} and A_0. Quartz was present as an impurity in the china clay, while rutile was added to CGC as a nucleating agent. Quartz dissolved at temperatures above 1400°C; rutile was undetected due to the addition of lesser amounts of CGC.

3.2 Microstructural characterization of phase assemblages

Petrographic examinations of thin sections under transmitted light showed a great variation in the respective microstructures with changes in phase assemblages described below.

3.2.1 Changes in cordierite phase

With an increase in CGC content in the raw mixes (> 15%) and at lower firing temperatures (1300°C), cordierite crystallized aided by TiO_2 nucleation. The cordierite crystals were euhedral in shape, having a bladed or tabular habit. They were identified by their colourless character under plane polarized light, exhibiting parallel extinction and negative optical character under crossed Nicols. They also showed cleavage planes parallel to the elongated axis (Fig. 2).

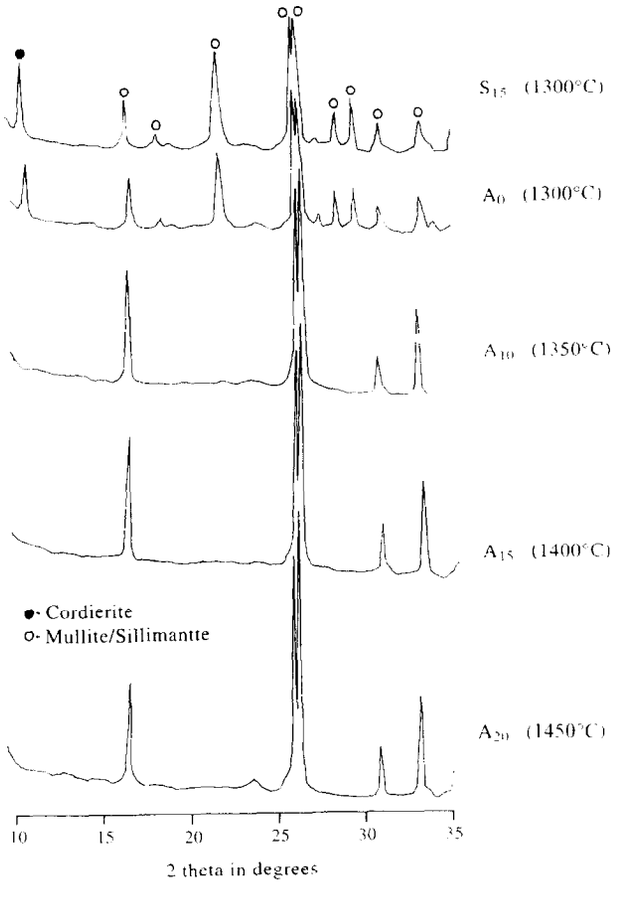

Fig. 1. XRD analysis of vitrified compositions.

With ≥25% CGC, more crystalline cordierite precipitated. It had a well-defined habit and sharp grain boundaries (Fig. 2). With less CGC (< 15%) and at higher firing temperature (1350°C, A_{10}) it dissolved while partially retaining its grain boundaries. At still higher temperatures (> 1400°C), cordierite dissolved completely into a Mg-rich liquid phase.

3.2.2 Formation of mullite

Mullite occurs in porcelain bodies in two morphologies. Besides the well-known needles (secondary mullite), it also occurs as a fine crypto-crystalline mass of scaly patches (primary mullite). Primary mullite is composed of aggregates of small mullite seeds, which might be as small as 100 Å. These are primary, as they form directly from clay: secondary mullite is formed from the melt by dissolution and recrystallization.

Primary mullite is susceptible to dissolution and recrystallization in the presence of the increased silica content of the glassy phase,[5] which in turn is influenced by the dissolution of finer quartz. Thus, mullite present in S_{15} (15% quartz) was better crystallized and dimensionally larger than in the absence of free quartz.

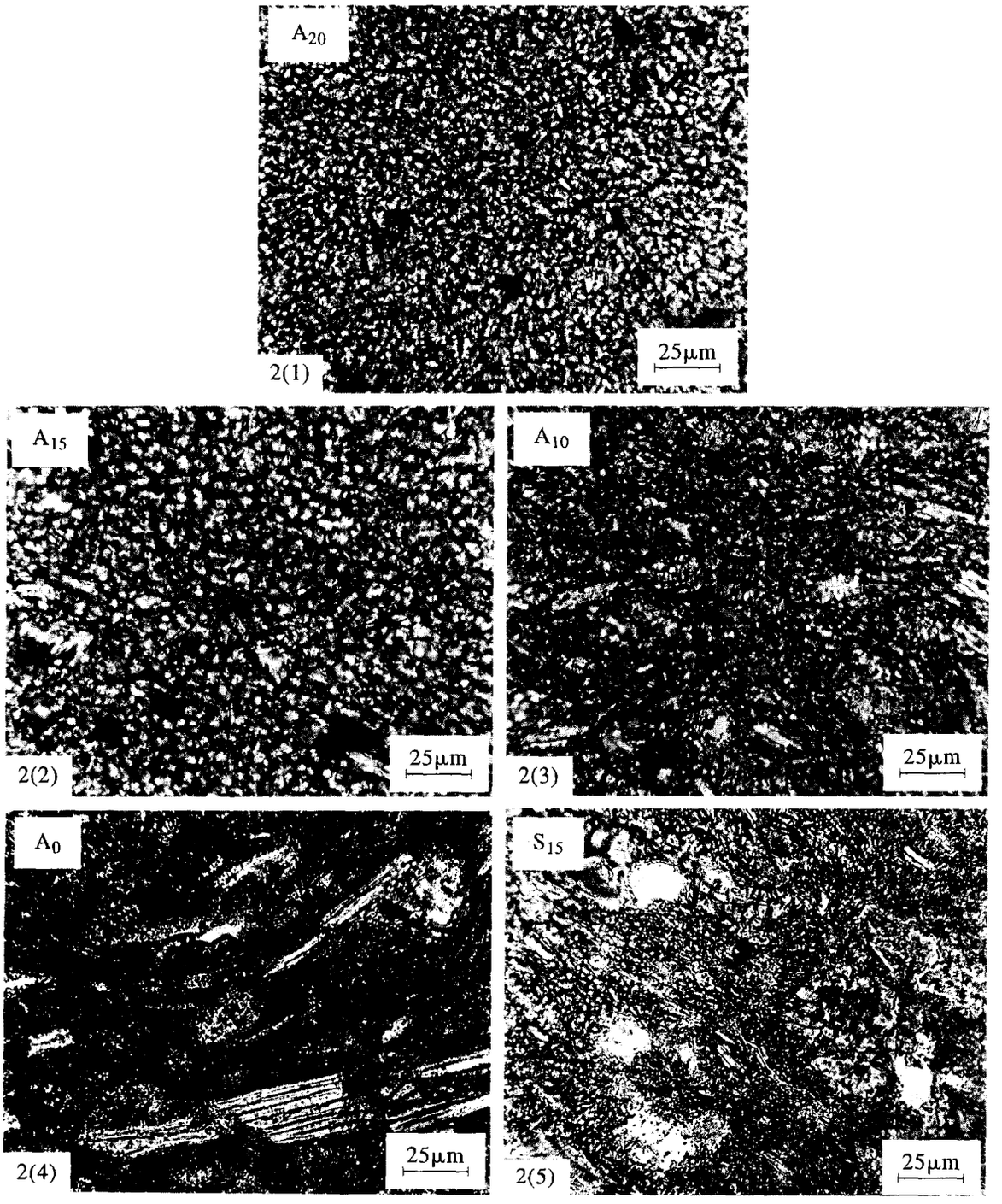

Fig. 2. Microstructural characterization of vitrified samples. Transmitted light, plane polarized.

A completely different microstructure was observed in samples with progressive alumina addition. All the primary mullite aggregates dissolved, subsequently recrystallizing as secondary acicular mullite (A_{10}) within a glassy matrix. This contradicts Schuller,[6] who stated that melts poor in silica do not attack primary mullite, even above 1350°C.

3.2.3 Modification of sillimanite sand

Sillimanite sand added in the present compositions was very finely ground (mean particle size $\simeq 4\,\mu m$). It could not be distinguished from the groundmass in the samples fired at 1300°C (S_{15}, A_0). However, in samples fired at and above 1350°C, sillimanite grains could be clearly distinguished from the glassy groundmass; under crossed Nicols it had a mottled appearance. The grains were almost euhedral in shape, with clear, well-defined boundaries. With increased firing temperature they tend to a botryoidal habit, with a sharp decrease in grain size.

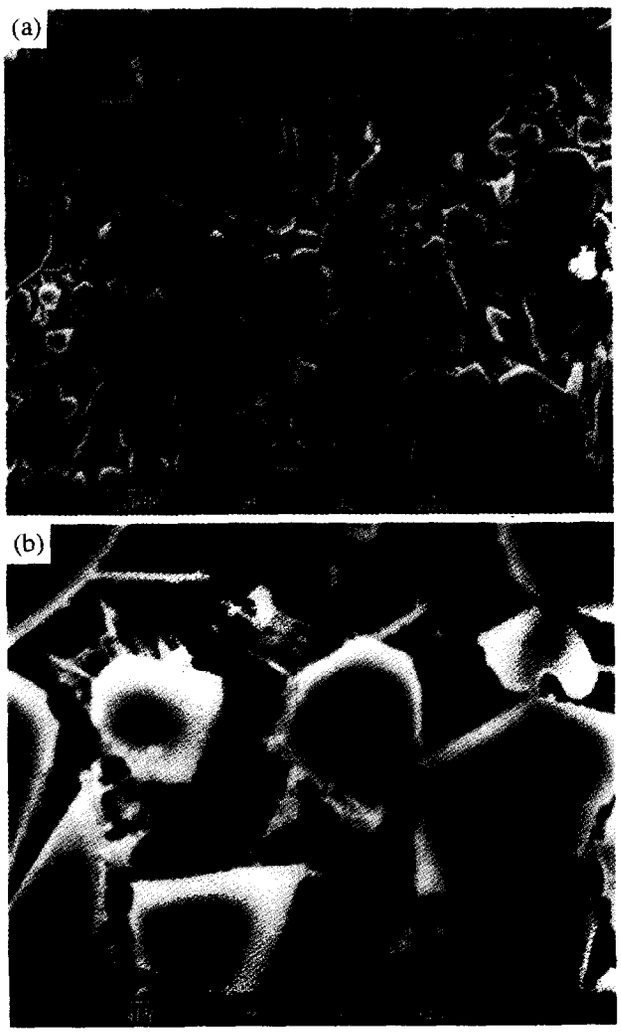

Fig. 3. Secondary electron image of A_{20} composition fired at 1450°C showing: (a) dissolution of sillimanite grains and (b) presence of fine mullite needles in the interstitial spaces.

3.3 Scanning electron probe micro-analysis

At around 1300°C, sillimanite sand grains did not reveal any change in size or shape. Grains were mainly elongated and angular. They did not show cracks, fissures or inclusions, inferring that they were unreacted. That the elongated grains were sillimanite was inferred from the elemental mapping of Si and Al, showing Al > Si: microprobe analysis confirmed them to be near theoretical sillimanite composition. However, the matrix was equally rich in Al and Si, with some Mg and Ti contributed from CGC, which had partially reacted.

During firing, the CGC melted and subsequently recrystallized as minute crystals in an amorphous matrix. Its nucleation was enhanced by the added TiO_2. Microprobe analysis of the minute secondary crystallites found that they were close to the theoretical cordierite composition.

Firing a composition of 50% clay, 25% sillimanite sand, 20% alumina and 5% CGC at 1450°C gave a microstructure of very fine needle-like structures in the regions between the interconnected structures (Fig. 3). These needles could only be detected by SEM. Closed pores formed from the interparticle space present during the initial compaction. Formation of necks between euhedral grains by solid state diffusion was also seen. SEPMA confirmed the needles as mullite and the interconnected microstructure to be nearly of theoretical sillimanite composition. The matrix composition was the same as that of A_{15}, with only an increase of Al content in place of Si due to increased addition of alumina in place of cordierite glass ceramic.

3.4 Role of microstructure on the strength

Figure 4 shows the variation in flexural strength on body composition, as shown in Table 2. With increasing alumina replacing CGC, the flexural strength increases. At 20% Al_2O_3, with an alumina:CGC ratio of 4, a flexural strength of 195 MPa was achieved, close to that of high alumina ceramics. This was due to suitable tailoring of initial particle size and processing parameters of the raw materials, resulting in a dense, mosaic microstructure of euhedral sillimanite grains embedded in a glassy matrix. The presence of fine mullite needles in the interstitial spaces of the grains also improves the strength. Complete wetting of the crystalline phases and absence of any Griffith cracks, due to volume expansion mismatch between the crystalline phase and the glassy matrix, were favourable for strength development. It was concluded that a

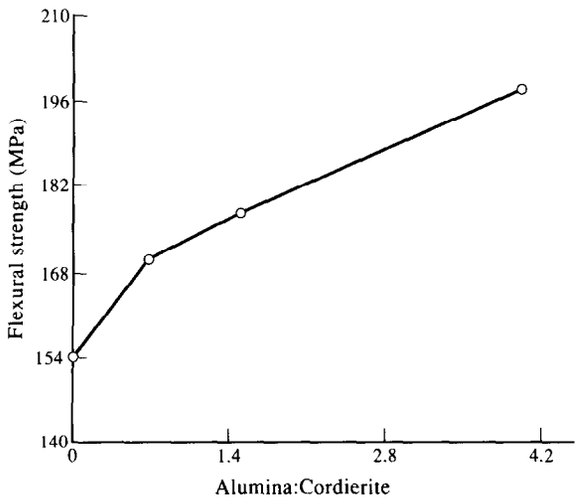

Fig. 4. Flexural strength of vitrified porcelains with increasing replacement of cordierite glass-ceramic by alumina.

suitable development of such a dispersion-strengthened glassy matrix would markedly increase the strength of porcelain compositions.

4 CONCLUSIONS

It has been shown that in a clay–sillimanite sand porcelain with a varying alumina/cordierite glass-ceramic ratio, no change in sillimanite sand takes place up to 1400°C. Above 1400°C dissolution sets in and the angular sillimanite tends to a more euhedral shape. At 1450°C mullite remains as very fine needles in the interstitial spaces of the sillimanite grains. The presence of a mosaic structure, with complete wetting of the crystalline phases by the dense glassy matrix and absence of any Griffith cracks, increased the mechanical strength.

ACKNOWLEDGEMENTS

The authors are grateful to Shri. D. K. Naskar for help rendered in specimen preparation. Thanks are also due to Dr Tapan Roy, DMRL, Hyderabad for SEM and SEPMA of the specimens. Financial assistance from the Council of Scientific & Industrial Research, Government of India, in the form of a research fellowship grant, is also gratefully acknowledged.

REFERENCES

1. MATTYASOVSKY-ZOLSNAY, L., Mechanical strength of porcelain. *J. Am. Ceram. Soc.*, **40** (1957) 299–306.
2. WARSHAW, S. I. & SEIDER, R., Comparison of strength of triaxial porcelain containing alumina and silica. *J. Am. Ceram. Soc.*, **50** (1967) 337–343.
3. BRADT, R. C., A high-tech approach to a traditional ceramic — the toughness of porcelain. In *Proc. Int. Symp. on Fine Ceramics*, Arita 86, 1986, pp. 15–22.
4. BLODGETT, W. E., High strength alumina porcelains. *Am. Ceram. Soc. Bull.*, **40** (1961) 74–77.
5. SCHULLER, K. H., Structure development in porcelain — I. *Ber. Deut. Keram. Ges.*, **38** (1961) 150–157.
6. SCHULLER, K. H., Structure development in porcelain — IV. *Ber. Deut. Keram. Ges.*, **40** (1963) 320–326.
7. PETROVA, V. Z. & AVGUSTINIK, A. I., The solution of alumina in feldspar porcelains. *Zh. Prikl. Khim.*, **32** (1959) 2788.
8. FLOYD, J. R., ROYCE, D. V. & LIPPMAN, A., Alumina versus flint in whiteware bodies. Internal report of Alumina Research Division, Reynolds Metals Company, Bauxite, Arkansas, 1966.